Hydrological Sciences Journal
Publication details, including instructions for authors and subscription information:
http://www.tandfonline.com/loi/thsj20

Climate change uncertainty in environmental flows for the Mekong River

J.R. Thompson[a], C.L.R. Laizé[b], A.J. Green[a], M.C. Acreman[b] & D.G. Kingston[c]

[a] Wetland Research Unit, UCL Department of Geography, University College London, Gower Street, London WC1E 6BT, UK

[b] Centre for Ecology and Hydrology, Wallingford, Oxfordshire OX10 8BB, UK

[c] Department of Geography, University of Otago, PO Box 56, Dunedin, New Zealand

Accepted author version posted online: 17 Sep 2013.Published online: 28 Feb 2014.

To cite this article: J.R. Thompson, C.L.R. Laizé, A.J. Green, M.C. Acreman & D.G. Kingston (2014) Climate change uncertainty in environmental flows for the Mekong River, Hydrological Sciences Journal, 59:3-4, 935-954, DOI: 10.1080/02626667.2013.842074

To link to this article: http://dx.doi.org/10.1080/02626667.2013.842074

Hydrological Sciences Journal – Journal des Sciences Hydrologiques, 59 (3–4) 2014
http://dx.doi.org/10.1080/02626667.2013.842074
Special issue: *Hydrological Science for Environmental Flows*

Climate change uncertainty in environmental flows for the Mekong River

J.R. Thompson[1], C.L.R. Laizé[2], A.J. Green[1], M.C. Acreman[2] and D.G. Kingston[3]

[1]*Wetland Research Unit, UCL Department of Geography, University College London, Gower Street, London WC1E 6BT, UK*
j.r.thompson@ucl.ac.uk

[2]*Centre for Ecology and Hydrology, Wallingford, Oxfordshire OX10 8BB, UK*

[3]*Department of Geography, University of Otago, PO Box 56, Dunedin, New Zealand*

Received 21 January 2013; accepted 22 July 2013; open for discussion until 1 September 2014

Editor Z.W. Kundzewicz

Citation Thompson, J.R., Laizé, C.L.R., Green, A.J., Acreman, M.C., and Kingston, D.G., 2014. Climate change uncertainty in environmental flows for the Mekong River. *Hydrological Sciences Journal*, 59 (3–4), 935–954.

Abstract A MIKE SHE model of the Mekong, calibrated and validated for 12 gauging stations, is used to simulate climate change scenarios associated with a 2°C increase in global mean temperature projected by seven general circulation models (GCMs). Impacts of each scenario on the river ecosystem and, hence, uncertainty associated with different GCMs are assessed through an environmental flow method based on the range of variability approach. Ecologically relevant hydrological indicators are evaluated for the baseline and each scenario. Baseline-to-scenario change is assessed against thresholds that define likely risk of ecological impact. They are aggregated into single scores for high and low flows. The results demonstrate considerable inter-GCM differences in risk of change. Uncertainty is larger for low flows, with some GCMs projecting high and medium risk at the majority of locations, and others suggesting widespread no or low risk. Inter-GCM differences occur along the main Mekong, as well as within major tributaries.

Key words environmental flows; climate change; uncertainty; MIKE SHE; Mekong

Incertitude liée au changement climatique sur les débits environnementaux du Mékong
Résumé Un modèle du Mékong de type MIKE SHE, calé et validé pour 12 stations de jaugeage, a été utilisé pour simuler des scénarios de changement climatique associés à une augmentation de 2°C de la température globale moyenne projetée par sept modèles climatiques globaux (MCG). Les impacts de chaque scénario sur l'écosystème de la rivière, et par conséquent l'incertitude associée aux différents MCG, ont été évalués à l'aide d'une méthode de débits environnementaux fondée sur l'approche de la « Gamme de variation ». Des indicateurs hydrologiques pertinents pour l'écologie ont été évalués pour la référence et pour chaque scénario. Le changement référence-scénario a été évalué par rapport à des seuils définissant le risque probable d'impact écologique. Ces indicateurs ont été agrégés en notations individuelles pour les crues et pour les étiages. Les résultats montrent des différences considérables entre MCG en terme de risque de changement. L'incertitude est plus élevée pour les débits d'étiage, avec quelques MCG projetant des risques élevés et moyens pour la plupart des sites et d'autres suggérant des risques faibles voire nuls. Les différences entre MCG se manifestent aussi bien le long du lit principal du Mékong que de ses principaux affluents.

Mots clefs débits environnementaux ; changement climatique ; incertitude ; MIKE SHE ; Mékong

INTRODUCTION

Southeast Asia's Mekong River is one of the most iconic rivers in the world. Like all river ecosystems, the Mekong's waters bring direct benefits to people, including water for public supply, power generation, food—such as rice—as well as fish and aquatic plants. Its flow of river water also has significant social and spiritual meaning to local communities and supports important species, such as the emblematic sub-population of the Irrawaddy dolphin

(*Orcaella brevirostris*) and the Mekong giant catfish (*Pangasianodon gigas*; Hogan *et al.* 2004). All of these attributes are commonly referred to as ecosystem services (Fischer *et al.* 2009, Maltby and Acreman 2011). The term "environmental flows" has been applied increasingly to describe the flow regime of a river required to maintain economically, socially and ecologically important ecosystem services (Dyson *et al.* 2003). However, the world's rivers are changing due to multiple pressures including land-use change, water diversions, dams and climate change, which will have implications for their ecosystem services (Millennium Ecosystem Assessment 2005, Vörösmarty *et al.* 2010).

Climate change represents a global pressure that may have profound implications for environmental flows. It is expected to impact the global hydrological cycle, with implications for both human use of water resources (Bates *et al.* 2008) and aquatic ecosystems (Poff *et al.* 2002). The common approach to assessing the potential hydrological impacts of climate change is to drive a hydrological model with climate projections derived through forcing general circulation models (GCMs) with emissions scenarios. Uncertainty is introduced at each stage of this process (Gosling *et al.* 2011). There is uncertainty in the definition of greenhouse gas emissions scenarios. Climate model structural uncertainty causes different GCMs to produce different projections for the same scenario. Uncertainty is also related to downscaling GCM projections to finer spatial and temporal scales for hydrological modelling. Hydrological models used to translate climatological changes to hydrological impacts add additional uncertainty. While GCM uncertainty has frequently been found to be the greatest source of uncertainty (e.g. Graham *et al.* 2007, Prudhomme and Davies 2009), that associated with other factors may not be negligible (Haddeland *et al.* 2011).

GCM uncertainty is often investigated by driving a hydrological model with climate projections from different GCMs for the same emissions scenario, and analysing differences between changes in, for example, simulated river flow (e.g. Singh *et al.* 2010, Kingston *et al.* 2011). It is far less common to extend the analysis to evaluate uncertainty in changes to environmental or ecological conditions, although examples do exist (e.g. Singh *et al.* 2011).

There is a range of methods for assessing river environmental flow requirements (Tharme 2003, Acreman and Dunbar 2004). Some are tailored to specific environments, such as freshwater flows to estuaries. Others incorporate different options for addressing the same issue: flow needs of river ecosystems. This may introduce further uncertainty into assessments of the impacts of climate change. Nevertheless, common themes are to define the response of ecosystems to flow change and to identify thresholds where ecological change may be significant. Many methods follow the natural flow paradigm (Poff *et al.* 1997) that assumes a river's flow regime, comprising key components of variability, magnitude, frequency, duration, timing and rate of change, is central to sustaining biodiversity and ecosystem integrity. All elements of the flow regime are important for some aspect of river ecosystems. For example, flow variability drives fish assemblage structure both directly, by influencing critical life history processes including spawning, migration and recruitment, and indirectly, by impacting floodplain connectivity (Nestler *et al.* 2012). Assessment of alteration of flow regimes from natural conditions has become a standard approach to environmental flow assessment (Poff *et al.* 2010). For example, the widely employed range of variability approach (RVA) uses indicators of hydrological alteration (IHAs), a statistical technique for comparing natural and altered flow regimes (Richter *et al.* 1996, 1997). This study employs a modified IHA approach (Laizé *et al.* 2013) and a MIKE SHE model (Thompson *et al.* 2013) to investigate implications of GCM uncertainty for environmental flows in the Mekong under a consistent magnitude of climate change.

THE MEKONG CATCHMENT

The Mekong is the largest river in Southeast Asia. It is the world's eighth largest in terms of annual discharge (475 km^3), 12th longest (~4350 km) and 21st largest by drainage area (795 000 km^2). The river originates in China's Tibetan Highlands and passes through or borders Burma, Laos, Thailand, Cambodia and Vietnam before discharging into the South China Sea (Fig. 1). The dominant climatic influence is the Asian monsoon. Over 90% of annual precipitation falls between mid-May and early October. River discharge begins to rise in May. Peak flows occur between August and October, whilst minimum flows are in March–April. In the upper catchment, snow storage and melt influence discharge considerably, although snow covers only ~5% of the total catchment during November–March and is negligible at other times.

Rapid development and population growth have driven agricultural expansion and deforestation, and are linked to increasing competition for water, water contamination by agriculture, industry and settlements, and unsustainable use of resources including fisheries

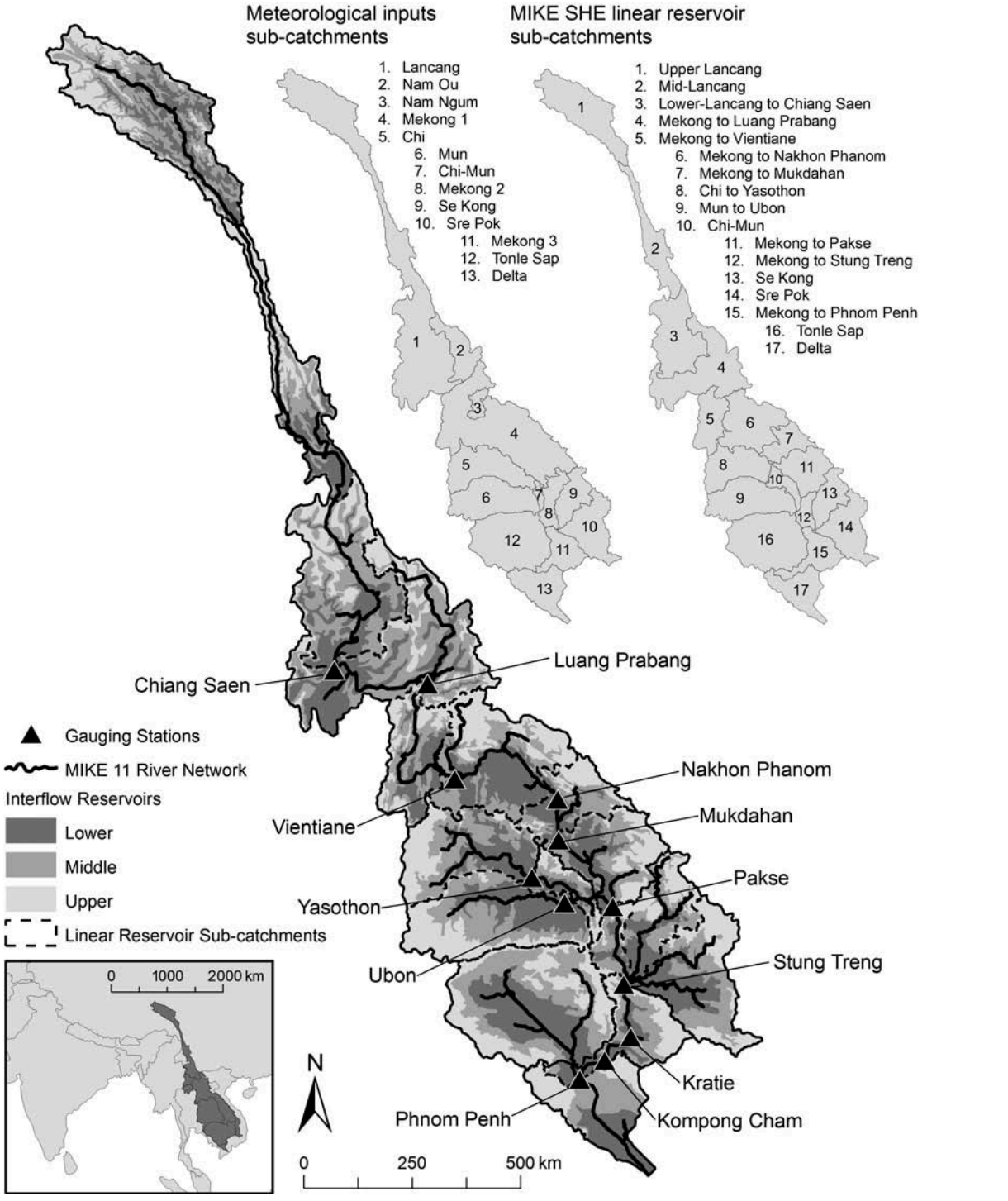

Fig. 1 The Mekong catchment and its representation within the MIKE SHE model including the distribution of linear reservoir sub-catchments, interflow reservoirs and meteorological inputs. The gauging stations within the MIKE 11 river network that were used for calibration and validation are also indicated.

(Kirby *et al.* 2010). With the population of the lower Mekong (i.e. downstream of the Lancang sub-catchment) projected to increase from 55 million in 2003 to 90 million by 2025 (MRC 2003), these pressures will increase. In addition, dams have already impacted on flow regimes, sediment flows and fisheries (Li and He 2008, Wang *et al.* 2011), and more are planned (Stone 2010, Ziv *et al.* 2012). Climate change will interact with such pressures, with potentially significant implications for environmental flows.

Changes in river flows may have significant ecological, economic and social consequences given the ecosystem services provided by the Mekong (e.g. Dugan *et al.* 2010). Of particular importance may be fisheries impacts. After the Amazon, the Mekong is the second largest in terms of aquatic diversity (Ferguson *et al.* 2011), with 279 new fish species being identified in the decade up to 2009 (WWF 2009). Mekong fisheries support around 300 million people (MRC 2003). The river produces around 2.5 million tonnes of fish annually, with an estimated economic value of US$1.4–1.9 billion. Hydrological factors including the magnitude, duration and timing of the annual flood strongly influence these fisheries (Baran and Myschowoda 2009). Similarly, the flood sustains huge agricultural productivity in areas including the Mekong Delta by providing water for rice fields, depositing fertile silt and by removing salty, acidic water (e.g. Hoa *et al.* 2008).

METHODS

Hydrological modelling

Here we employ a model developed using MIKE SHE, a comprehensive, highly flexible hydrological model offering a range of process descriptions (Graham and Butts 2005). MIKE SHE has a modular structure, with components for the primary processes of the land phase of the hydrological cycle. It has been applied to a range of hydrological systems, from small catchments (Al-Khudhairy *et al.* 1999, Sahoo *et al.* 2006, Thompson 2012), through medium and large catchments (Singh *et al.* 2010, 2011), to major international river basins (Andersen *et al.* 2001, Stisen *et al.* 2008).

Thompson *et al.* (2013) provide a detailed account of the MIKE SHE Mekong model, so only an overview is given herein. Table 1 summarizes the model components and data employed within them. The conceptual, semi-distributed, linear reservoir saturated zone method was employed due to its lower data requirements. Figure 1 shows the 17 groundwater sub-catchments and their division into 51 interflow reservoirs.

The model's 10 km × 10 km computational grid was a compromise between logistically appropriate computation times and representation of catchment attributes. Channel flow was simulated using the MIKE 11 one-dimensional hydraulic model. Dams were not included as many extant dams were completed after the calibration period (see below) and the focus here is GCM-related uncertainty. All MIKE 11 branches were coupled to MIKE SHE and received overland flow, interflow and baseflow.

Precipitation, temperature and potential evapotranspiration (PET) were distributed using 13 sub-catchments of an earlier SLURP model (Kingston *et al.* 2011; Fig. 1). Gridded monthly precipitation from the University of Delaware (UDel) global precipitation data set was spatially averaged for each meteorological sub-catchment and stochastically disaggregated to a daily resolution (Arnell 2003). This study employed revised UDel data, cf. the original Mekong model as described by Thompson *et al.* (2014). The same procedure was applied to mean temperature derived from the CRU TS 3.0 data set. Monthly gridded Linacre PET (Dent *et al.* 1988, Schulz 1989) was calculated using climate variables from the CRU TS 3.0 data set, averaged across each meteorological input sub-catchment and distributed evenly through the month on a daily basis.

Calibration was undertaken using observed discharge data obtained from the Mekong River Commission for 12 gauging stations that provide the most complete records (Fig. 1). The period 1961–1990 was used for calibration, although records from three stations did not cover the full period and discharges for Kratie were computed from Pakse discharge following Institute of Hydrology (1988). Calibration parameters were time constants for the interflow and baseflow reservoirs, linear reservoir dead storage proportions and, in meteorological sub-catchments with large elevation ranges, precipitation lapse rates. The snowmelt degree-day coefficient was varied during calibration of the Lancang at Chiang Saen. Calibration was undertaken in a downstream sequence. A preliminary automatic multiple objective calibration was employed (e.g. Madsen 2000). This evaluated model performance at the model time step (maximum 48 hours). However, because daily baseline meteorological data were produced through the stochastic disaggregation of monthly data, there was a disconnect between the daily meteorological inputs and observed daily discharge. Consequently, model performance was improved through manual parameter modification, with performance statistics calculated using monthly mean discharges. Model performance was evaluated using the Nash-Sutcliffe coefficient (NSE; Nash and Sutcliffe 1970), the correlation coefficient (r) and the percentage deviation in simulated mean flow from the observed mean flow (Dv). The performance classification scheme of Henriksen *et al.* (2008) was employed. The period 1991–1998 was used for validation

Table 1 Summary of key data employed within each component of the coupled MIKE SHE/MIKE 11 model of the Mekong. The numeric engines (see Graham and Butts 2005) employed for the overland flow, unsaturated zone, saturated zone and snowmelt modules are also indicated.

Model component	Key inputs	Data sources/derivation
Model domain	Catchment extent	Derived using the USGS GTOPO30 DEM (Kite 2000)
Topography	Topography	Extracted from the USGS GTOPO 30 DEM
Land use/vegetation	Vegetation distribution	Spatial distribution of nine land-cover classes derived from the USGS Global Land Cover Characterization data set
	Leaf area indexes	Kite (2000)
	Root depths	Kelliher *et al*. (1993), Jackson *et al.* (1996) and a DHI (2009) vegetation properties file
Overland flow: modelled using the 2D finite-difference method	Manning's *M* for overland flow resistance	Spatially distributed according to land cover. Values taken from the literature (Chow 1959, Thompson *et al.* 2004, Vieux 2004, Sahoo *et al*. 2006, Thompson 2012)
Unsaturated zone: modelled using the two-layer water balance method	Soil textural classes	Spatial distribution of four textural classed derived from the FAO Digital Soil Map of the World (FAO 1990)
	Soil hydraulic characteristics	Clapp and Hornberger (1978), Carsel and Parrish (1988), Marshall *et al*. (1996)
Saturated zone: modelled using the conceptual, linear reservoir method	Spatial distribution of groundwater sub-catchments	The catchment was divided into 17 groundwater sub-catchments (Fig. 1) based on the locations of the 12 gauging stations used for model calibration/validation, the major tributaries of the Mekong and topography
	Spatial distribution of interflow reservoirs	Each groundwater sub-catchment was divided into three interflow reservoirs, based on topography
	Spatial distribution of baseflow reservoirs	Each groundwater sub-catchment was divided into an upper (faster) and a lower (slower) baseflow reservoir
Catchment meteorology: precipitation, evapotranspiration and degree-day snowmelt modules	13 meteorological sub-catchments	Derived through topographic analysis of the USGS GTOPO30 DEM (Kite 2000)
	Precipitation, potential evapotranspiration (PET) and temperature data	See text for meteorological data sources
MIKE 11 one-dimensional hydraulic model for simulating channel flow (using Muskingum routing)	Plan of the main river channels	Derived through topographic analysis of the USGS GTOPO30 DEM (Kite 2000)
	Synthetic cross sections for different stream orders	Established using surveyed cross sections (Shopea 2003, Mekong River Commission: http://ffw.mrcmekong.org/) and stream width measurements taken in Google Earth Pro
	Manning's *n* for bed resistance	Chow (1959)

although data for two stations do not extend to this period, whilst records for others varied in length.

Climate change scenarios

Monthly resolution climate change scenarios for precipitation, temperature and Linacre PET were generated for an arbitrary 30-year period using the ClimGen spatial scenario generator (Arnell and Osborn 2006). For a given GCM, ClimGen scales the pattern of climate change up and down in magnitude using the assumption that the spatial pattern of change, expressed as a change per unit of global mean temperature, is constant for that GCM. As described by Thompson *et al*. (2013), scenarios were generated for a prescribed 2°C increase in global mean temperature (relative to 1961–1990), a hypothesized threshold of dangerous climate change (Todd *et al.* 2011), for seven GCMs: CCCMA CGCM31, CSIRO Mk30, IPSL CM4, MPI ECHAM5, NCAR CCSM30, UKMO HadGEM1 and UKMO HadCM3. Different GCMs enable an exploration of the implications of GCM uncertainty for changes in discharge, and hence environmental flows. Monthly gridded scenario precipitation and temperature were stochastically disaggregated to a daily resolution and spatially averaged for the meteorological input sub-catchments. Gridded monthly scenario Linacre PET was derived using ClimGen output. As for baseline PET, gridded monthly totals were spatially averaged at the sub-catchment scale and evenly distributed through each month on a daily basis.

Assessment of environmental flows and ecological risk

Environmental flows for the baseline and each climate change scenario were determined using a modified version of the ecological risk due to flow alteration (ERFA) screening method (Laizé *et al*. 2013). This is based on the RVA using IHAs, a technique for defining ecologically appropriate limits of hydrological change (Richter *et al*. 1996, 1997). It assumes that some organism or community will have exploited every niche created by the complexity of the flow hydrograph and its interaction with the landscape. If a river ecosystem is adapted to baseline hydrological conditions, then an impact causing departure from these conditions is likely to alter the ecosystem. The likelihood of alteration increases as the hydrological regime departs further from baseline conditions. The risk will move from none to low to medium to high as thresholds of flow alteration are exceeded. Ecologically important flow regime characteristics (magnitude, duration, timing, frequency and rate of change) can be indexed by indicators describing key flow regime properties.

In common with IHA/RVA, ERFA employs indicators describing the flow regime that are calculated for the baseline (1961–1990) and each scenario. Unlike IHA/RVA, which uses daily flow variables, ERFA employs monthly variables termed monthly flow regime indicators (MFRIs). This approach is appropriate in the present study given the focus on monthly mean discharges. Presenting results of the departure from baseline of every MFRI would involve a prohibitively large amount of information, especially for a large catchment such as the Mekong. To enable ready interpretation, ERFA aggregates information as a simple colour-coded risk classification based on how many indicators differ from the baseline by more than a set threshold (Laizé *et al*. 2013).

Olden and Poff (2003) reviewed 171 currently available hydrological indices. They identified nine distinct components of the flow regime and concluded that the number of indices depends on the particular type of flow regime. The present study uses a subset of MFRIs consistent with Olden and Poff's strategy. Hydrological variables (one value per year of the simulation period per site) are used to derive indicators capturing the magnitude and variability of each variable as one value for the whole simulation period for each site. Magnitude is described by the median (50th percentile), and variability by the interquartile range (IQR, i.e. difference between 25th and 75th percentiles) of the annual variables. Indicators associated with the timing of flood and minimum flow (MFRI 3 and 6, Table 2) differ since they are defined by the months (1–12) when peak and low flows occur and are more meaningfully summarized by their mode. Eight indicators were derived based on five hydrological variables (Table 2): three medians, three IQR and two modes. Three indicators (MFRI 1–3) are associated with high flows and five (MFRI 4–8) with low flows.

Table 2 Monthly flow regime indicators (MFRIs).

Hydrological variables (one per year)	MFRI[c] (one per period)	Flow type	Regime characteristics
Number of months above threshold[a]	Median (1)	High flows	Magnitude, frequency
	IQR[d] (2)		
Month of maximum flow (1–12)	Mode (3)	High flows	Timing
Number of months below threshold[b]	Median (4)	Low flows	Magnitude, frequency
	IQR (5)		
Month of minimum flow (1–12)	Mode (6)	Low flows	Timing
Number of periods of at least 2 months duration with flow below threshold[b]	Median (7) IQR (8)	Low flows	Magnitude, frequency, duration

Notes
[a]Threshold: Q5 (95th percentile) from the 1961–1990 calibration period.
[b]Threshold: Q95 (5th percentile) from the 1961–1990 calibration period.
[c]Indicator identification number between brackets.
[d]Inter-quartile range.

Indicators were evaluated for 217 q-points (where MIKE 11 calculates discharge) along the river as defined by the MIKE 11 model. The Tonle Sap and Delta sub-catchments were excluded as the lack of suitable observed discharge data prevented model calibration below Phnom Penh. Absolute differences between indicators for each scenario and the baseline were calculated for each q-point. The median or IQR MFRIs for the scenarios were considered to depart substantially from the baseline if they differed by more than 30%. Significant changes to the mode indicators were defined as changes larger than one month.

For practicality, ease of display and interpretation at the whole catchment scale, differences were aggregated via a colour-coding system adapted from Laize *et al.* (2013). Given the different number of indicators for high and low flows, two distinct colour codes were defined. In the case of high flows

(MFRI 1–3), a q-point was assigned blue (no risk), green (low risk), amber (medium risk) or red (high risk of ecological change) when the number of indicators differing from the baseline was 0, 1, 2 or 3, respectively. In the case of low flows (MFRI 4–8), the corresponding number of differences in indicators was 0 (no risk), 1 (low risk), 2–3 (medium risk) and 4–5 (high risk). The low risk category is intentionally set to one indicator differing from the baseline in both cases.

RESULTS

Calibration and validation

Performance statistics for the calibration and validation periods are shown in Table 3. Model performance for the calibration period is generally classed as "excellent" (20 out of 24 performance statistics). Values of r are above or close to 0.95 at 10 of the 12 gauging stations. Generally, similar performance is indicated for the validation period, although at some stations with limited observations (e.g. Stung Treng and those in the Chi and Mun sub-catchments) model performance is much weaker.

Figure 2 shows observed and simulated river regimes for all 12 stations for the calibration period. These demonstrate good agreement between Chiang Saen and Pakse. Below Pakse, there is slight overestimation of ascending limb discharges leading to Dv for the calibration period falling below the "excellent" category at Kompong Chang ("very good") and Phnom Penh ("fair"). Performance for the Chi and Mun sub-catchments is weak in comparison to other gauging stations (NSE: "poor" and "fair", respectively) although Dv values are classed as "excellent" (Table 3). Simulated peak seasonal discharges are underestimated, whilst rising and descending limbs are largely well reproduced. Thompson *et al*. (2013) concluded that the model was fit for the purpose of assessing GCM-related climate change uncertainty, especially for the calibration period that

Table 3 Model performance statistics based on mean monthly discharge for 12 gauging stations within the Mekong catchment for the calibration period (1961–1990 unless stated otherwise) and for 10 gauging stations for the validation period (1991–1998 unless stated otherwise). Model performance indicators are taken from Henriksen *et al*. (2008).

Station	Period	Dv (%)		NSE		r
Mekong at Chiang Saen	Calibration: 1961–1990	+0.88	☆☆☆☆☆	0.888	☆☆☆☆☆	0.943
	Validation: 1991–Jun 1997	–4.47	☆☆☆☆☆	0.822	☆☆☆☆	0.831
Mekong at Luang Prabang	Calibration: 1961–1990	+3.82	☆☆☆☆☆	0.892	☆☆☆☆☆	0.947
	Validation: 1991–1997	2.11	☆☆☆☆☆	0.863	☆☆☆☆☆	0.864
Mekong at Vientiane	Calibration: 1961–1990	+4.86	☆☆☆☆☆	0.900	☆☆☆☆☆	0.951
	Validation: 1991–1996	5.35	☆☆☆☆	0.908	☆☆☆☆☆	0.913
Mekong at Nakhon Phanom	Calibration: 1961–1990	+4.14	☆☆☆☆☆	0.910	☆☆☆☆☆	0.955
	Validation: 1991–Nov 1995	1.33	☆☆☆☆☆	0.907	☆☆☆☆☆	0.908
Mekong at Mukdahan	Calibration: 1961–1990	+3.58	☆☆☆☆☆	0.907	☆☆☆☆☆	0.953
	Validation: 1991–1995	3.59	☆☆☆☆☆	0.921	☆☆☆☆☆	0.925
Mekong at Pakse	Calibration: 1961–1990	+3.13	☆☆☆☆☆	0.901	☆☆☆☆☆	0.951
	Validation: 1991–1998	4.75	☆☆☆☆☆	0.890	☆☆☆☆☆	0.900
Mekong at Stung Treng	Calibration: 1961–1969	+3.97	☆☆☆☆☆	0.924	☆☆☆☆☆	0.963
	Validation: 1991–1993	–11.59	☆☆☆	0.902	☆☆☆☆☆	0.916
Mekong at Kratie	Calibration: 1961–1990	+1.20	☆☆☆☆☆	0.901	☆☆☆☆☆	0.950
	Validation: 1991–1998	1.33	☆☆☆☆☆	0.891	☆☆☆☆☆	0.902
Mekong at Kompong Cham	Calibration: 1964–Mar 1974	+6.18	☆☆☆☆	0.904	☆☆☆☆☆	0.954
	—	—	—	—	—	—
Mekong at Phnom Penh	Calibration: 1961–Mar 1974	+13.03	☆☆☆	0.866	☆☆☆☆☆	0.951
	—	—	—	—	—	—
Chi at Yasothon	Calibration: 1961–1990	+0.88	☆☆☆☆☆	0.494	☆☆	0.712
	Validation: 1991–1995	19.95	☆☆☆	–0.312	☆	0.175
Mun at Ubon	Calibration: 1961–1990	+0.34	☆☆☆☆☆	0.550	☆☆☆	0.750
	Validation: 1991–1993	–0.32	☆☆☆☆☆	0.136	☆	0.309

Performance indicator	Excellent ☆☆☆☆☆	Very good ☆☆☆☆	Fair ☆☆☆	Poor ☆☆	Very poor ☆
Dv	<5%	5–10%	10–20%	20–40%	>40%
NSE	>0.85	0.65–0.85	0.50–0.65	0.20–0.50	<0.20

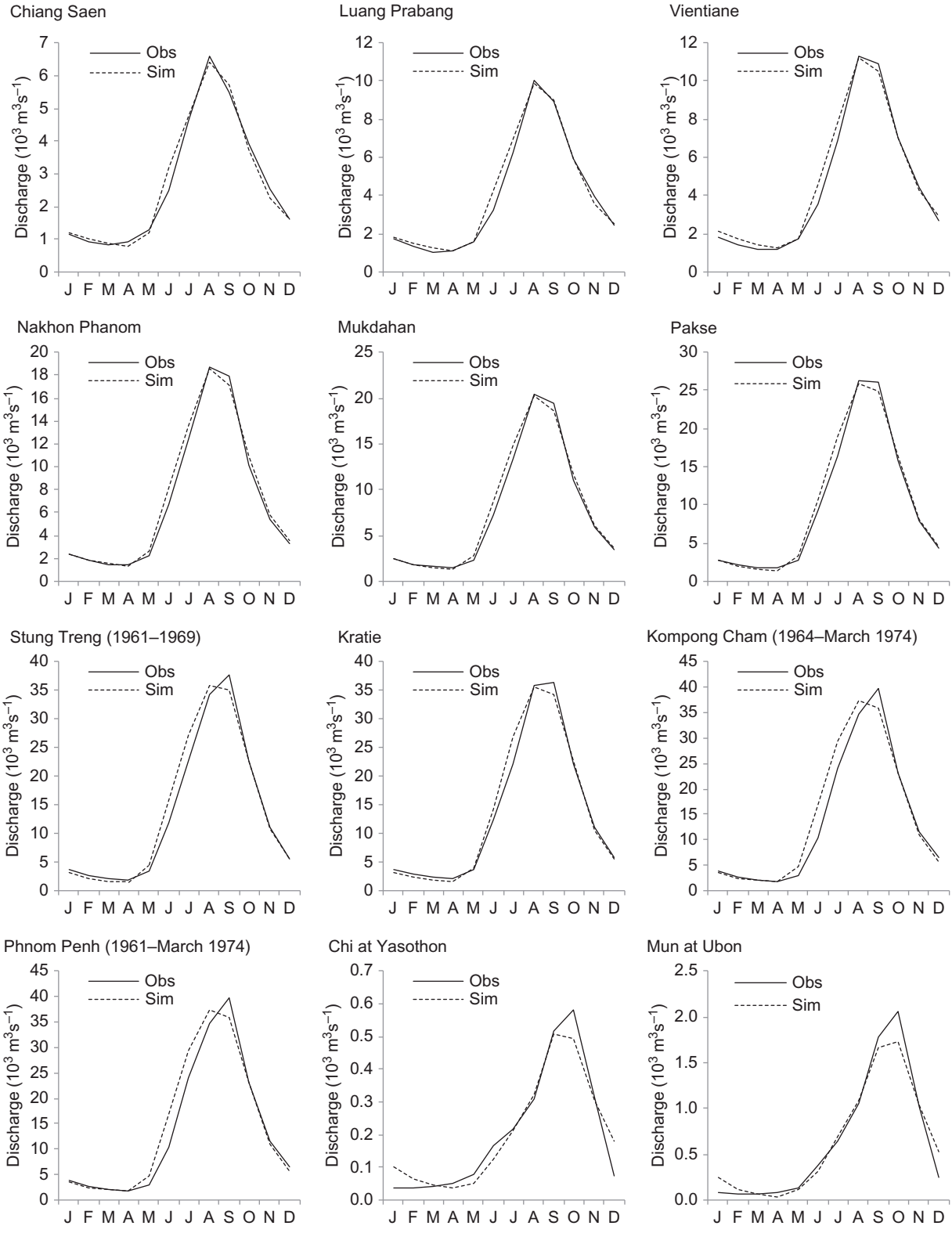

Fig. 2 Observed and simulated river regimes for 12 gauging stations within the Mekong catchment for the calibration period (1961–1990, unless indicated otherwise).

provides baseline conditions. Performance statistics are superior to those obtained for a SLURP model for the same period (Kingston *et al.* 2011) and compare very favourably with some previous models of the Mekong (e.g. Hapuarachchi *et al.* 2008, Västilä *et al.* 2010).

Table 4 Mean annual precipitation and potential evapotranspiration (PET) for the baseline (mm) and changes (%) for the climate change scenarios for representative sub-catchments within the Mekong catchment. (Numbers in brackets refer to the meteorological inputs sub-catchments identified in Fig. 1. Shaded cells indicate negative changes compared to the baseline.)

Parameter	Scenario	Lancang (1)	Mek. 1 (4)	Chi (5)	Mun (6)	Mek. 2 (8)	Se Kong (9)	Sre Pok (10)	Mek. 3 (11)
Precipitation	Baseline	1052.8	1855.8	1272.3	1313.6	2213.2	2432.5	2055.3	1870.3
	CCCMA	10.1	10.2	12.3	10.2	8.4	5.2	1.9	5.3
	CSIRO	–4.6	–4.6	–3.3	–2.9	–2.8	–2.8	–2.9	–1.3
	HadCM3	10.1	1.0	–0.1	–0.4	–1.1	–2.1	–4.5	–3.0
	HadGEM1	5.9	–3.7	–6.1	–4.8	–1.2	2.9	3.9	1.0
	IPSL	–5.2	–1.1	–0.1	–0.1	0.6	–0.4	1.3	–0.4
	MPI	3.6	7.0	10.2	10.3	8.8	6.6	7.6	12.2
	NCAR	8.5	9.1	5.0	3.5	1.9	3.5	3.7	5.3
PET	Baseline	1765.6	1923.0	2363.6	2336.5	1813.0	1728.5	1695.9	1770.3
	CCCMA	11.7	12.3	13.1	12.7	12.5	12.7	12.3	12.5
	CSIRO	14.6	15.7	15.9	15.2	15.2	14.9	14.2	14.3
	HadCM3	12.9	13.9	13.3	13.2	14.7	14.8	14.8	15.1
	HadGEM1	12.4	12.1	10.3	10.3	12.4	13.0	12.7	12.5
	IPSL	15.9	15.7	15.3	14.2	14.3	13.9	12.8	13.2
	MPI	13.6	13.6	13.3	12.9	13.4	13.5	13.1	13.2
	NCAR	11.3	10.9	11.1	10.6	11.4	11.1	10.7	10.3

Climate change

Changes in climate Table 4 presents baseline annual precipitation and PET for eight representative meteorological sub-catchments, and percentage changes for each GCM for the 2°C prescribed increase in global mean temperature. Thompson *et al*. (2013) provide a detailed account of these changes. Mean monthly precipitation and PET for the baseline and each scenario are shown for four representative sub-catchments in Fig. 3. Changes in temperature are not presented since time-series of temperature are only relevant within the Lancang, the one sub-catchment with significant snowmelt. Changes in mean annual temperature for this sub-catchment range from +2.3°C (CCCMA) to +2.9°C (IPSL).

Changes in annual precipitation vary between GCMs: CCCMA, MPI and NCAR show increases for all sub-catchments, with CCCMA and NCAR exhibiting the greatest increases in upstream sub-catchments, whilst downstream increases are greater for MPI; CSIRO shows decreased annual precipitation within all sub-catchments, with the largest decreases upstream; annual precipitation declines for IPSL in all but three south-central sub-catchments (Chi-Mun, Mekong 2 and Sre Pok); HadCM3 simulates increased precipitation over the four northernmost sub-catchments and decreases elsewhere; and HadGEM1 projects increases for the two northernmost sub-catchments and three southern sub-catchments (Se Kong, Sre Pok and Mekong 3).

Intra-annual patterns of precipitation change vary between GCMs: CSIRO, IPSL and MPI exhibit unimodal changes with increases for CSIRO and IPSL concentrated around September (decreases for the majority of the year). Increases are concentrated in May–November for MPI. Other GCMs show a bimodal pattern of change, with the greatest increases occurring at different times depending on GCM.

Inter-GCM differences in PET are smaller than those for precipitation (Table 4, Fig. 3). All GCMs simulate increases in annual PET across the catchment. The smallest increases are associated with NCAR and HadGEM1. There is a systematic geographical pattern for the GCMs producing the largest PET changes. In the four northernmost sub-catchments (sub-catchments 1–4), IPSL simulates the largest increases. In the middle catchment (sub-catchments 5–9), larger changes are associated with CSIRO, whilst in the lower Mekong (sub-catchments 10–13), HadCM3 provides the greatest increases.

Changes in river discharge Table 5 shows mean, Q_5 and Q_{95} (discharges exceeded 5% and 95% of the time, respectively) discharges derived from monthly simulated flow at eight representative gauging stations for the baseline period, and percentage changes for each 2°C GCM scenario. Figure 4 shows baseline and scenario river regimes for these stations. As described in detail by Thompson *et al*. (2013), discharge changes show substantial inter-GCM differences. Of the three GCMs for which precipitation increases in all sub-catchments, two (CCCMA and NCAR) result in increased mean discharge at all stations. For CCCMA, increases are

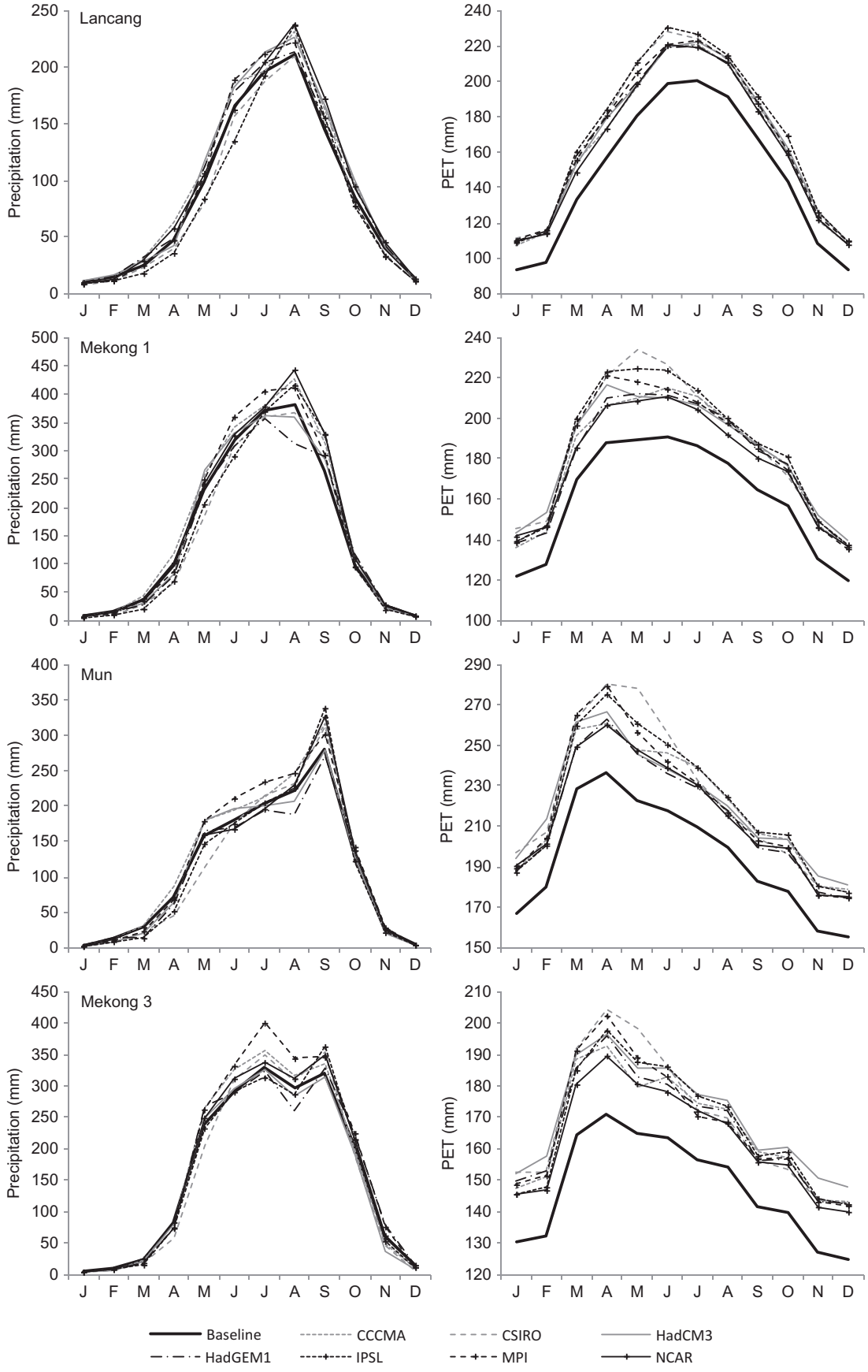

Fig. 3 Mean monthly precipitation and PET for the baseline and under 2°C prescribed warming for seven GCMs (note the different *y*-axis scales).

Table 5 Mean, Q_5 and Q_{95} discharges ($m^3 s^{-1}$) for the baseline and changes from these values (%) under 2°C prescribed warming for seven GCMs at eight gauging stations within the Mekong catchment (shaded cells indicate negative changes compared to the baseline).

Discharge	Scenario	Chiang Saen	Luang Prabang	Vientiane	Mukdahan	Pakse	Kratie	Phnom Penh	Ubon
Mean	Baseline	2735.3	4132.4	4740.9	7874.4	10 144.8	13 579.8	13 942.4	638.4
	CCCMA	7.3	6.9	7.4	8.3	9.0	7.2	7.0	11.0
	CSIRO	–21.2	–21.6	–21.1	–17.7	–16.4	–14.7	–14.4	–11.4
	HadCM3	11.3	9.9	7.8	3.7	1.4	–1.7	–2.1	–8.2
	HadGEM1	0.2	–3.5	–5.6	–8.5	–10.4	–9.1	–9.0	–20.6
	IPSL	–19.7	–18.1	–16.8	–12.6	–10.6	–9.4	–9.4	–3.0
	MPI	–2.3	–1.0	0.2	2.6	4.9	5.6	5.9	16.5
	NCAR	8.7	12.4	12.6	12.7	11.2	8.2	8.0	2.9
Q_5	Baseline	6920.5	10 523.9	12 135.5	21 635.8	28 188.2	38 302.0	39 560.1	2037.3
	CCCMA	–3.5	0.2	–1.1	8.1	10.2	7.4	8.0	18.6
	CSIRO	–19.6	–19.0	–16.4	–13.5	–12.8	–10.9	–11.0	–1.9
	HadCM3	4.9	4.0	3.5	–1.4	–2.5	–4.9	–5.3	–3.7
	HadGEM1	–4.8	–6.8	–6.8	–11.8	–14.9	–15.6	–14.8	–11.9
	IPSL	–13.7	–7.8	–10.2	–6.5	–1.6	–3.3	–3.8	10.1
	MPI	–4.8	1.3	1.0	2.9	6.1	6.5	6.5	19.3
	NCAR	6.5	11.0	9.2	12.3	7.7	6.8	6.2	11.6
Q_{95}	Baseline	767.9	1092.6	1234.0	1345.2	1438.4	1560.9	1583.1	23.9
	CCCMA	7.5	13.0	13.4	13.5	16.3	14.3	13.1	22.0
	CSIRO	–23.2	–23.5	–21.4	–18.2	–17.7	–18.2	–19.1	–15.0
	HadCM3	12.9	11.0	9.0	11.4	9.2	9.0	8.2	–6.3
	HadGEM1	–1.6	–2.6	–2.9	–4.4	–4.1	–3.9	–4.7	–17.5
	IPSL	–21.9	–18.3	–16.9	–16.4	–15.7	–15.9	–16.2	–9.4
	MPI	–3.2	–0.6	–0.8	–0.6	0.3	–0.2	–1.3	6.8
	NCAR	11.4	17.0	17.7	20.3	19.5	17.7	16.6	3.2

relatively uniform along the main Mekong. The greater increase for the Mun at Ubon is representative of sub-catchments in the central part of the Mekong such as the Chi and Chi-Mun. Whilst increases in Q_5 and Q_{95} are also seen at most stations, decreases in Q_5 are seen at Chiang Saen and Vientiane. All three discharge indicators increase at all stations for NCAR. In most cases, changes are greater than for CCCMA.

Mean discharge in upstream parts of the catchment declines for MPI. Further downstream, it increases, with the magnitude of changes increasing in a downstream direction, although changes on the Mekong are smaller than for CCCMA and NCAR. Below Chiang Saen, increases in discharge are concentrated in the wet season, resulting in higher Q_5, whilst decreases in the post-peak recession result in modest declines in Q_{95} at most stations. CSIRO and IPSL show decreases in mean, Q_5 and Q_{95} discharges along the length of the Mekong (Q_5 increases at Ubon and Yasothon for IPSL). Reductions are larger for CSIRO and are greatest in upstream locations for both GCMs, and generally decline in magnitude with distance downstream.

For HadGEM1, there is a marginal (0.2%) increase in mean discharge at Chiang Saen, although both Q_5 and Q_{95} decrease. Further downstream, all three discharge measures decline. The magnitude of reductions in mean discharge increases with movement downstream to Pakse: they then stabilize at around 9%; Q_5 and Q_{95} show a similar pattern. River regimes show that reductions in discharge are concentrated in August and September, the period of peak flows.

For the HadCM3 scenario, mean discharge increases along the Mekong as far as Pakse and then declines. Modest increases in dry-season flows are reflected in increased Q_{95} at all gauging stations on the Mekong (declines for Ubon). Increases in Q_5 are restricted to upstream stations, although mean discharge in August (peak flows) declines throughout the catchment. From Mukdahan downstream, mean discharges in both August and September decline.

Changes in ecological risk Figures 5 and 6 show for each GCM, MIKE 11 q-points colour-coded according to the risk of ecological alteration associated with changes in high and low flows, respectively. For each sub-catchment above Phnom Penh, Table 6 indicates the percentage of q-points in each risk category for the high-flow MFRIs; corresponding figures for low-flow MFRIs are shown in Table 7. Consistent with inter-GCM differences in simulated river discharge, there is considerable spatial variation in the environmental flows represented

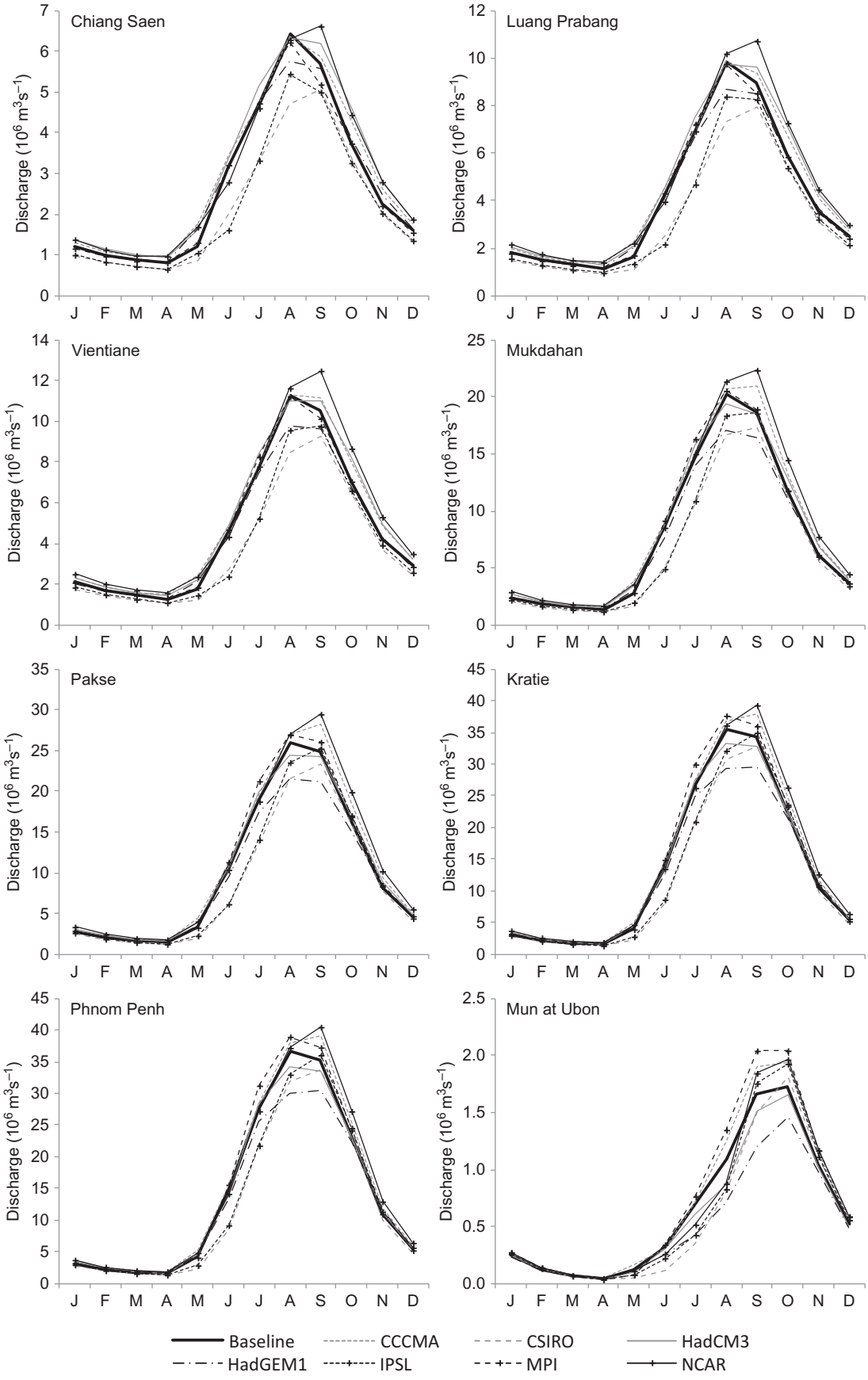

Fig. 4 River regimes for the baseline and under 2°C prescribed warming for seven GCMs at eight gauging stations within the Mekong catchment.

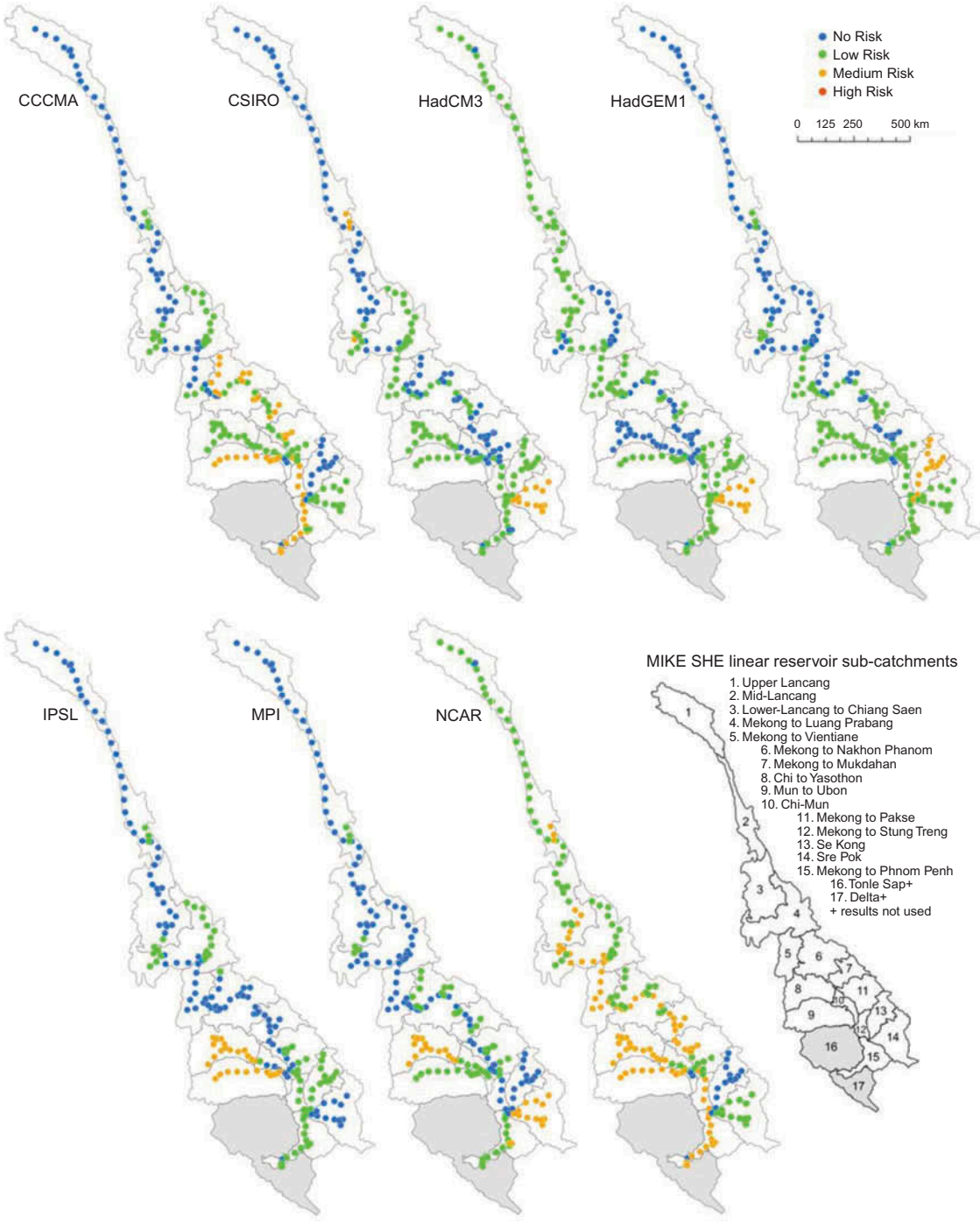

Fig. 5 Risk of hydrological change for high-flow monthly flow regime indicators at all MIKE 11 q-points within the Mekong model for 2°C prescribed warming for seven GCMs.

by the MFRIs. This variation and the relative order of risk are different between high- and low-flow indicators and between GCMs, representing overall uncertainty in projections.

For high flows, no GCMs project a high risk of ecological alteration at any q-points (Table 6); thus there is some certainty in this result. Across all GCMs, the most likely outcome is no or low risk of ecological change (at least 50% of q-points classed in these two categories). The results for NCAR demonstrate the highest risk with 48% of q-points classed as medium risk, more than twice as many as any other GCM. This relatively large risk is associated with increases in high flows (Table 5 and Fig. 4). The CCCMA model, which also projects increases in mean discharge throughout the Mekong and in Q_5

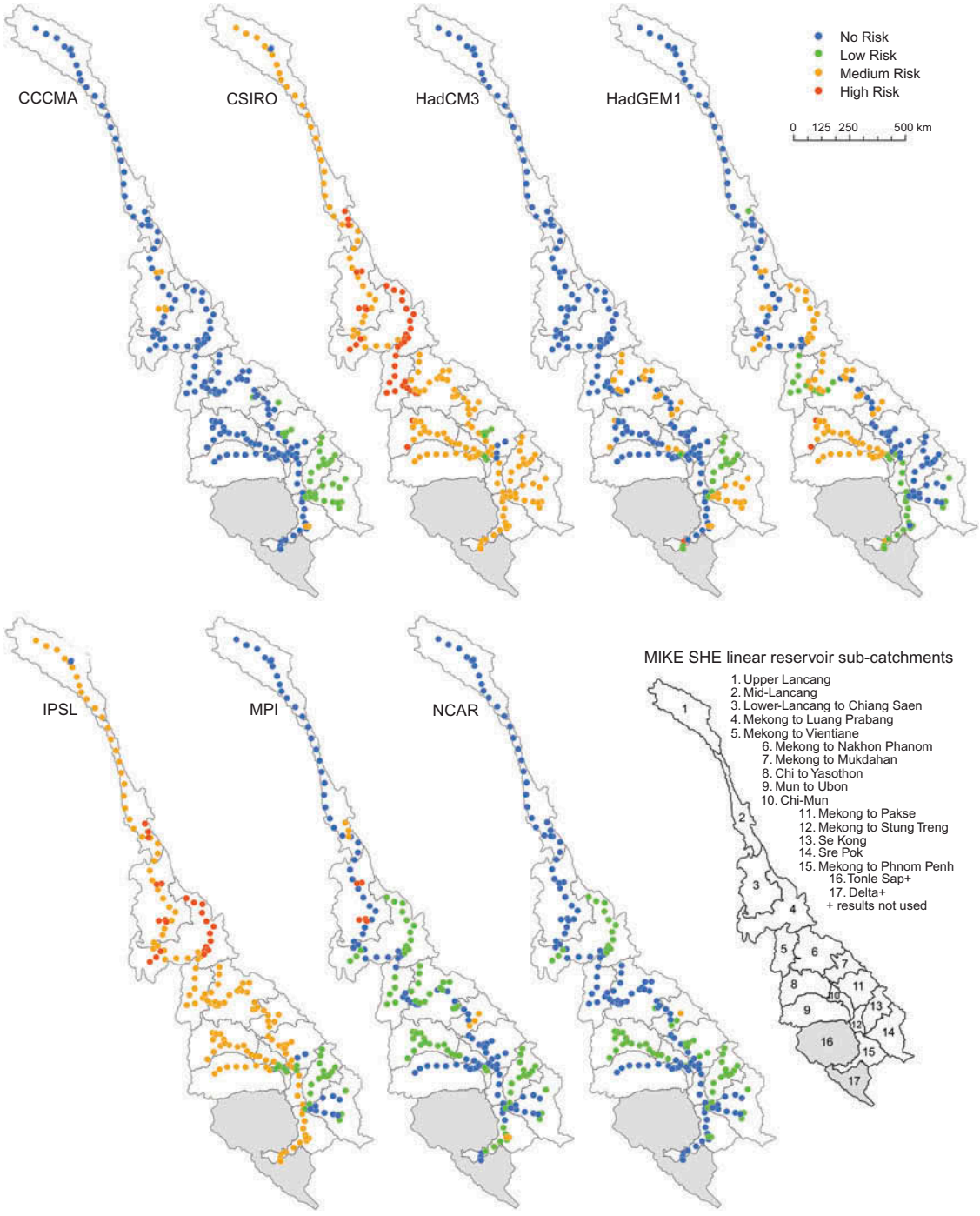

Fig. 6 Risk of hydrological change for low-flow monthly flow regime indicators at all MIKE 11 q-points within the Mekong model for 2°C prescribed warming for seven GCMs.

at most stations, is second highest in terms of medium risk for high flows (24% of q-points); IPSL, closely followed by MPI, have the largest number of q-points (55% and 54%, respectively) classed as no risk. Both have 31% classified as low risk, whilst only 14% and 15%, respectively, fall within the medium risk class. This similar risk is despite differences in the direction of change in high flows, increases at most locations for MPI and decreases for IPSL (Table 5). Similar results are evident for the remaining three GCMs (CSIRO, HadCM3 and HadGEM1). They have smaller numbers (6–9%) of q-points classed as medium risk compared to IPSL and MPI, but a larger number (50–65%) classed as low risk. A consistent 91–94% of q-points are within the lowest two risk categories for these three GCMs.

Table 6 Percentage of high-flow MFRIs within each sub-catchment classified according to risks of hydrological change for each GCM (sub-catchment numbers refer to the MIKE SHE linear reservoir sub-catchments identified in Fig. 1).

	Risk[a]	Sub-catchment															
		1	2	3	4	5	6	7	8	9	10	11	12	13	14	15	Total
q-points	—	14	18	15	26	11	23	7	16	10	11	17	5	14	15	15	217
CCCMA	No risk	100	83	87	35	73	17	0	0	0	18	0	0	100	0	7	37
	Low	0	17	13	65	27	26	57	100	0	64	59	0	0	100	13	39
	Medium	0	0	0	0	0	57	43	0	100	18	41	100	0	0	80	24
	High	0	0	0	0	0	0	0	0	0	0	0	0	0	0	0	0
CSIRO	No risk	100	83	87	19	18	57	71	0	0	55	82	0	0	0	20	41
	Low	0	0	13	77	82	43	29	100	100	45	18	100	100	0	80	50
	Medium	0	17	0	4	0	0	0	0	0	0	0	0	0	100	0	9
	High	0	0	0	0	0	0	0	0	0	0	0	0	0	0	0	0
HadCM3	No risk	14	0	0	65	0	30	57	100	0	82	59	0	0	0	7	30
	Low	86	100	100	35	100	70	43	0	100	18	41	100	100	0	93	63
	Medium	0	0	0	0	0	0	0	0	0	0	0	0	0	100	0	7
	High	0	0	0	0	0	0	0	0	0	0	0	0	0	0	0	0
HadGEM1	No risk	100	83	87	77	0	57	29	0	0	18	41	0	0	0	7	40
	Low	0	17	13	23	100	43	71	100	100	82	59	100	0	100	93	54
	Medium	0	0	0	0	0	0	0	0	0	0	0	0	100	0	0	6
	High	0	0	0	0	0	0	0	0	0	0	0	0	0	0	0	0
IPSL	No risk	100	83	87	35	100	96	100	0	0	45	35	0	0	100	7	55
	Low	0	17	13	65	0	4	0	0	0	9	65	100	100	0	93	31
	Medium	0	0	0	0	0	0	0	100	100	45	0	0	0	0	0	14
	High	0	0	0	0	0	0	0	0	0	0	0	0	0	0	0	0
MPI	No risk	100	83	87	92	100	43	57	0	0	0	53	80	100	0	0	54
	Low	0	17	13	8	0	57	43	0	100	100	47	20	0	0	87	31
	Medium	0	0	0	0	0	0	0	100	0	0	0	0	0	100	13	15
	High	0	0	0	0	0	0	0	0	0	0	0	0	0	0	0	0
NCAR	No risk	14	0	0	0	0	0	0	0	0	18	0	0	100	0	7	9
	Low	86	83	60	58	18	57	0	0	0	55	41	0	0	100	0	43
	Medium	0	17	40	42	82	43	100	100	100	27	59	100	0	0	93	48
	High	0	0	0	0	0	0	0	0	0	0	0	0	0	0	0	0

[a] Risk based on number of MFRIs differing by more than 30% from the baseline: 0 (no risk), 1 (low risk), 2 (medium risk) and 3 (high risk).

Low-flow MFRIs (Table 7) demonstrate that, for some GCMs, changes at some q-points are classified as high risk, but in most cases the number of q-points is relatively small. The CSIRO model followed by IPSL shows the highest risk of alteration to low flows. These GCMs have 20% and 11%, respectively, of q-points classed as high risk. With 64% and 69%, respectively, of q-points classified as medium risk, the majority (94% and 80%) of locations are projected to experience alterations to low flows in the top two risk classes. These alterations are associated with the projected catchment-wide decreases in low flows (Table 5). Much smaller risks of alterations to low flows result for CCCMA and NCAR (associated with catchment-wide increases in low flows, Table 5) with, respectively, 81% and 70% of q-points classed as no risk of change. For NCAR, the remaining 30% are classified as low risk, so that all locations fall within the lowest two risk categories. This is almost repeated for CCCMA with the exception of seven q-points (3%) that are classified as medium risk. The remaining three GCMs (HadCM3, HadGEM1 and MPI) display a dominant trend for relatively low risk of change. For example, 94% of q-points are classified as either no or low risk for MPI. For HadCM3, this figure is 82% (although 18% are medium risk), whilst for HadGEM1, the combined no/low risk classes account for 66% of q-points with one-third being classified as medium risk.

Assessment of the overall risk of alteration to environmental flows can be obtained by combining high- and low-flow MFRIs. CSIRO followed by IPSL projects the highest overall risk of ecological change. For CSIRO, 51.5% of the combined high- and low-flow MFRIs for the q-points are in the top two risk categories (high risk: 10%, all associated with low flows; medium risk: 41.5%). For IPSL, this figure is 47% (high risk: 5.5%, again all low flows; medium risk: 41.5%). The lowest overall risk is associated with MPI, HadCM3 and CCCMA. For MPI, only 10.5% of the combined high- and low-flow MFRIs for all q-points are within the top two

Table 7 Percentage of low-flow MFRIs within each sub-catchment classified according to risks of hydrological change for each GCM (sub-catchment numbers refer to the MIKE SHE linear reservoir sub-catchments identified in Fig. 1).

	Risk[a]	Sub-catchment															
		1	2	3	4	5	6	7	8	9	10	11	12	13	14	15	Total
q-points	—	14	18	15	26	11	23	7	16	10	11	17	5	14	15	15	217
CCCMA	No risk	100	100	67	100	100	96	86	100	100	100	76	100	0	0	87	81
	Low	0	0	0	0	0	4	14	0	0	0	24	0	100	100	0	16
	Medium	0	0	33	0	0	0	0	0	0	0	0	0	0	0	13	3
	High	0	0	0	0	0	0	0	0	0	0	0	0	0	0	0	0
CSIRO	No risk	14	0	0	0	0	0	0	0	0	0	24	0	0	0	0	3
	Low	0	0	0	0	0	0	0	0	0	18	24	0	0	0	0	3
	Medium	86	83	67	27	0	83	100	88	100	82	53	100	100	100	100	74
	High	0	17	33	73	100	17	0	13	0	0	0	0	0	0	0	20
HadCM3	No risk	100	100	100	100	100	43	57	88	100	55	100	100	0	0	60	73
	Low	0	0	0	0	0	0	0	0	0	9	0	0	100	0	20	9
	Medium	0	0	0	0	0	57	43	13	0	36	0	0	0	100	13	18
	High	0	0	0	0	0	0	0	0	0	0	0	0	0	0	7	0
HadGEM1	No risk	100	94	67	42	9	17	57	0	0	0	82	0	100	73	7	47
	Low	0	6	0	0	73	26	0	0	0	18	18	100	0	27	87	19
	Medium	0	0	33	58	18	57	43	88	100	82	0	0	0	0	7	33
	High	0	0	0	0	0	0	0	13	0	0	0	0	0	0	0	1
IPSL	No risk	14	0	0	0	0	0	0	0	10	18	12	0	0	73	0	8
	Low	0	0	0	0	0	0	0	0	0	55	12	0	100	27	0	12
	Medium	86	83	67	42	100	100	100	100	90	27	76	100	0	0	100	69
	High	0	17	33	58	0	0	0	0	0	0	0	0	0	0	0	11
MPI	No risk	100	83	67	42	55	35	57	0	100	73	100	100	0	73	47	58
	Low	0	0	0	58	45	65	0	100	0	27	0	0	100	27	40	36
	Medium	0	17	0	0	0	0	43	0	0	0	0	0	0	0	13	4
	High	0	0	33	0	0	0	0	0	0	0	0	0	0	0	0	2
NCAR	No risk	100	100	100	42	100	96	57	0	100	55	65	100	0	73	87	70
	Low	0	0	0	58	0	4	29	100	0	45	35	0	100	27	13	30
	Medium	0	0	0	0	0	0	14	0	0	0	0	0	0	0	0	0
	High	0	0	0	0	0	0	0	0	0	0	0	0	0	0	0	0

[a] Risk based on number of MRFIs differing by more than 30% from the baseline: 0 (no risk), 1 (low risk), 2–3 (medium risk) and 4–5 (high risk).

risk categories, 56% are classed as no risk and 89.5% are classified within the bottom two risk classes. For HadCM3 and CCCMA, 87.5% (no risk: 51.5%, low risk: 36%) and 86.5% (no risk: 59%, low risk: 27.5%), respectively, are in the lowest two risk classes. Both HadGEM1 and NCAR show intermediate results with 20% and 24%, respectively, in the top two risk categories and 80% and 76% in the bottom two risk classes.

Figures 5 and 6 show limited spatial consistency in the risk of ecological change. Results for NCAR, for example, demonstrate that some risk of alteration to high flows occurs throughout the catchment with the exception of the Se Kong (sub-catchment 13), for which no risk of alteration is projected for all q-points (Fig. 5). Along the main Mekong, there is a switch from low risk to medium risk at a point within the Lower Lancang above Chiang Saen (sub-catchment 3). For CCCMA, upper reaches of the Mekong show no risk; the switch to low risk occurs within sub-catchment 5 and then to medium risk below Pakse (sub-catchment 12). IPSL and MPI show no risk of alteration in high flows along most of the main Mekong (until Pakse and Stung Treng, respectively). Low and medium risk for high flows is limited to tributaries but results are inconsistent (Fig. 5). For example, both GCMs show medium risk throughout the Chi (sub-catchment 8) but the Mun (sub-catchment 9) shows medium risk for IPSL and low risk for MPI. Similarly, for the Sre Pok (sub-catchment 14), IPSL suggests no risk of change to high flows, whilst MPI projects medium risk.

Similar inter-GCM differences are evident in the spatial distribution of low-flow MFRIs (Fig. 6). For example, CSIRO projects medium risk of change throughout most of the river network. There is a concentration of high risk within the tributary joining the Mekong within sub-catchment 4 (as well as in small sub-catchments upstream) and then along the Mekong to Vientiane. IPSL shows similar results, although high risk of change does not extend to the main Mekong. In contrast, CCCMA shows

predominantly catchment-wide no risk with the exception of small tributaries and most notably the southern Se Kong and Sre Pok sub-catchments (sub-catchments 13 and 14, respectively) for which consistent low risk is projected. Similarly, for NCAR no risk of change in low-flow MRFIs is shown along the main Mekong. However, where some risk of change is demonstrated, all of low risk, it occurs in different sub-catchments to CCCMA (e.g. the Chi and the tributary joining the Mekong in sub-catchment 4), whilst no risk of change is indicated for most of the Sre Pok.

DISCUSSION AND CONCLUSIONS

This study further substantiates the previously demonstrated (Thompson *et al*. 2013) ability of the MIKE SHE model to reproduce observed river discharge throughout the Mekong. It has highlighted major differences in projected precipitation (and to a lesser extent PET) from seven GCMs for the same climate change scenario. This uncertainty is reflected in simulated Mekong discharge. Earlier assessments of the hydrological impacts and associated uncertainty of projections from the different GCMs have been extended using the ERFA screening method. This permits the risk of alteration of the river ecosystem resulting from hydrological change to be determined and provides a means of assessing GCM-related uncertainty for projections of future environmental flows.

The results demonstrate the critical importance of GCM-related uncertainty for assessing climate change impacts on environmental flows, with direct links clearly apparent from uncertainty in GCM projections to simulated discharge and, in turn, environmental flows. Assessment of uncertainty for the Mekong under a 2°C increase in global mean temperature across seven GCMs indicates that changes in ecologically relevant flow indicators could range from negligible to disastrous. Although only representing a subset of CMIP-3 GCMs, there is some indication that there are higher risks associated with low-flow changes compared to high-flow changes. Whilst no high-flow indices are classed as high risk, low-flow indices for some locations are classified as high risk for some GCMs. High-flow indicators for at least 50% of MIKE 11 q-points are classed as either no or low risk for all GCMs. Inter-GCM uncertainties in high-flow alterations do, however, exist with NCAR and, to a lesser extent CCCMA, suggesting widespread medium risk of alterations (due to increasing high flows), that is not replicated for other GCMs. For low flows, different GCMs (CSIRO and IPSL) are associated with higher risk. In both cases, the majority of q-points are classified in the top two risk categories. Other GCMs (CCCMA and NCAR) have a majority of q-points classed as no risk, and most if not all of the others as low risk. Uncertainty of low-flow impacts is therefore greater than that of high flows. The overall risk of change (combined risks to high and low flows) shows similar inter-GCM differences with some GCMs (CSIRO) having a small majority of indicators in the top two risk categories, and others (MPI, HadCM3 and CCCMA) a large majority in the bottom two classes. Spatial patterns of risk of alteration to high and low flows vary between GCMs. Inter-GCM differences occur both along the main Mekong as well as within its major tributaries.

Many organisms and biological communities in the Mekong are dependent on river flows and may be influenced by the changes in environmental flows that have been demonstrated. Given their previously described ecological, economic and social importance, fish are a key example. Commercially valuable fish are generally divided between two types: black and white fish (Welcomme 2001). Black fish, which in the Mekong include climbing perch (*Anabas testudineus*), clarias catfishes (e.g. *Clarias batrachus*) and snakehead (*Channa striata*) inhabit low oxygen, slow moving, shallow waters. They spend most of their lives in lakes and swamps on floodplains in the dry season, moving between permanent and seasonal habitats during the flood season (Poulsen *et al*. 2002a). Flood flows that inundate the floodplain and connect it to the river are thus critically important for these fish species. White fish, which include Cyprinids such as *Cyclcheilichthys enoplos* and *Cirrhinus microlepis*, as well as river catfish (Pangasiidae family), inhabit well-oxygenated, fast moving habitats in the main river channel for most of the year, relying on deep pool refuges during the dry season (Poulsen *et al*. 2002b). The widespread risk of alterations to low flows due to declines in discharge for the CSIRO and IPSL GCMs could be associated with a reduction in the availability of these refuge habitats during low water periods. White fish move into flooded areas during the monsoon season and subsequently return to the river as floodwaters recede. The seasonally inundated floodplains are the main fish production sites of the Mekong (Sverdrup-Jensen 2002) as they are rich in nutrients and provide refuge habitat away from floods in the main river channels. The largest risks of alteration to high

flows (for NCAR and CCCMA), which are associated with increasing high flows, may increase floodplain habitat. Where high flows are projected to decline (e.g. for CSIRO, HadCM3, HadGEM1 and IPSL), the magnitude of risk is generally low, although reductions in floodplain extent or the duration of inundation could be expected. Grey fish are an intermediate group between black and white fish (Welcomme 2001) and undertake short migrations between floodplain and adjacent rivers and/or permanent and seasonal water bodies within the floodplain (Chanh *et al*. 2001, Welcomme 2001). Some species migrate upstream to spawn at the start of the flood season and then rely on the river current to bring offspring to the downstream rearing habitats at the end of the flood. Consequently the timing of floods, so that they coincide with the breeding season, is vital to these species.

Other aquatic species display similar dependencies on hydrological conditions. For example, the Mekong's Irrawaddy dolphin population, which is currently less than 100 individuals, requires deep pool habitats, especially during the low-flow season, which, as previously noted, CSIRO and IPSL suggest may decline. Furthermore, the Siamese crocodile (*Crocodylus siamensis*) is thought to be sensitive to hydrological changes and its decline has been partially attributed to flow alterations caused by dams (Simpson and Bezuijen 2010). People living within the Mekong River system generate many other sources of food and income from other aquatic organisms, such as freshwater crabs, shrimp, snakes, turtles and frogs, that have requirements for certain hydrological conditions.

Thus it can be seen that magnitude and timing of floods is important for maintaining pools, fish migration and habitat connectivity, whilst sufficiently large low flows are required to maintain the more sensitive white fish species. Consequently, disruption of the hydrological regime by climate change, indexed by alterations in MFRIs, is likely to have significant implications for the river ecosystem and the services it provides to local people. However, because different parts of the river ecosystem have different flow requirements, and at present these are not known in sufficient detail, the broad-scale ERFA approach adopted in this paper is considered appropriate as it examines all aspects of the flow regime, each of which will be exploited by some organism or community.

The focus of the current study is inter-GCM uncertainty and its impacts on projected Mekong River discharge and, in turn, the risk of alteration to environmental flow conditions. As noted above, extension of the impacts of GCM-related uncertainty to environmental flows is relatively rare. To our knowledge, this is the first basin-wide assessment of the uncertainty in changing environmental flow conditions, as indicated by IHAs, associated with projections from different GCMs for a major river system in Southeast Asia. Other factors, most notably dam construction, but also widespread deforestation (e.g. Lacombe *et al.* 2010), will further modify river flow. For example, Lauri *et al.* (2012) investigated the impact of existing, under construction and planned hydropower reservoirs on Mekong River discharge. Their results suggested that dams might have a larger impact than climate change, with reductions in flood peaks at Kratie of 5–24% being projected. Conversely, high-flow flows increased by between 25% and 160%. Clearly the operation of these reservoirs will act to modify the risks of alterations to environmental flows demonstrated in the current study.

The combination of potentially catastrophic impacts on fish production and biodiversity (e.g. Ziv *et al*. 2012) of dams and climate change related alterations to the flow regime suggest major changes for the Mekong River ecosystem in the future. Investigation of the cumulative impacts, and their uncertainty, of climate change, dams and land-cover modifications upon environmental flows would be an invaluable extension of research on the Mekong River system. This could include further assessments of the uncertainty associated with the application of existing alternative hydrological models of the Mekong (e.g. Johnston and Kummu 2012) to the same scenarios. Thompson *et al*. (2013) have demonstrated that this is an additional source of uncertainty. Determining the precise nature of ecological impacts projected by such hydrological modelling studies would require detailed assessment of flow requirements of different species and their interactions in the food web.

Acknowledgements We thank Mac Kirby and an anonymous reviewer for their comments.

Funding The present study develops earlier research supported by a grant from the UK Natural and Environmental Research Council under the Quantifying and Understanding the Earth System (QUEST) programme (Ref. NE/E001890/1) and by its National Capability funding to the Centre for Ecology and Hydrology.

REFERENCES

Acreman, M.C. and Dunbar, M.J., 2004. Defining environmental river flow requirements—a review. *Hydrology and Earth System Sciences*, 8, 861–876.

Al-Khudhairy, D., *et al*., 1999. Hydrological modelling of a drained grazing marsh under agricultural land use and the simulation of restoration management scenarios. *Hydrological Sciences Journal*, 44, 943–971.

Andersen, J., Refsgaard, J.C., and Jensen, K.H., 2001. Distributed hydrological modelling of the Senegal River Basin—model construction and validation. *Journal of Hydrology*, 247, 200–214.

Arnell, N.W., 2003. Effects of IPCC SRES* emissions scenarios on river runoff: a global perspective. *Hydrology and Earth System Sciences*, 7, 619–641.

Arnell, N.W. and Osborn, T., 2006. *Interfacing climate and impacts models in integrated assessment modelling*. Tyndall Centre for Climate Change Research Technical Report 52. Southampton and Norwich: Tyndall Centre for Climate Change Research.

Baran, E. and Myschowoda, C., 2009. Dams and fisheries in the Mekong Basin. *Aquatic Ecosystem Health and Management*, 12, 227–234.

Bates, B.C., *et al*., eds., 2008. *Climate change and water*. Technical Paper of the Intergovernmental Panel on Climate Change. Geneva: IPCC Secretariat.

Carsel, R.F. and Parrish, R.S., 1988. Developing joint probability distributions of soil water retention characteristics. *Water Resources Research*, 24, 755–769.

Chanh, S., Chhuon, C.K., and Valbo-Jorgensen, J., 2001. Lateral migration between Tonle Sap River and its floodplain. *In*: K.I. Matics, ed. *Proceedings of the third technical symposium on Mekong Fisheries*, 8–9 December 2000 Mekong Conference Series No 1. Phnom Penh: Mekong River Commission, 102–111.

Chow, V.T., 1959. *Open channel hydraulics*. New York: McGraw-Hill.

Clapp, R.B. and Hornberger, G.M., 1978. Empirical equations for some soil hydraulic properties. *Water Resources Research*, 14, 601–604.

Dent, M.C., Schultze, R.E., and Angus, G.R., 1988. *Crop water requirements, deficits and water yield for irrigation planning in southern Africa.* Report 118/1/88. Pretoria: Water Research Commission.

DHI, 2009. *MIKE SHE technical reference*. Horsholm: DHI Water and Environment.

Dugan, P.J., *et al*., 2010. Fish migration, dams, and loss of ecosystem services in the Mekong Basin. *Ambio*, 39, 344–348.

Dyson, M., Bergkamp, G., and Scanlon, J., eds., 2003. *Flow—the essentials of environmental flows*. Cambridge: IUCN.

FAO, 1990. *FAO-UNESCO soil map of the world: revised legend, world soil resources report 60*. Rome: Food and Agriculture Organization of the United Nations.

Ferguson, J.W., *et al*., 2011. Potential effects of dams on migratory fish in the Mekong River: lessons from the Fraser and Columbia rivers. *Environmental Management*, 47, 141–159.

Fischer, B., Turner, R.K., and Morling, P., 2009. Defining and classifying ecosystem services for decision making. *Ecological Economics*, 68, 643–653.

Gosling, S.N., *et al*., 2011. A comparative analysis of projected impacts of climate change on river runoff from global and catchment-scale hydrological models. *Hydrology and Earth System Sciences*, 15, 279–294.

Graham, D.N. and Butts, M.B., 2005. Flexible, integrated watershed modelling with MIKE SHE. *In*: V.P. Singh and D.K. Frevert, eds. *Watershed models.* Boca Raton, FL: CRC Press, 245–272.

Graham, L.P., Andréasson, J., and Carlsson, B., 2007. Assessing climate change impacts on hydrology from an ensemble of regional climate models, model scales and linking methods—a case study on the Lule River basin. *Climatic Change*, 81, 293–307.

Haddeland, I., *et al*., 2011. Multi-model estimate of the global water balance: setup and first results. *Journal of Hydrometeorology*, 12, 869–884.

Hapuarachchi, H.A.P., *et al*., 2008. Investigation of the Mekong River basin hydrology for 1980–2000 using the YHyM. *Hydrological Processes*, 22, 1246–1256.

Henriksen, H.J., *et al*., 2008. Assessment of exploitable groundwater resources of Denmark by use of ensemble resource indicators and a numerical groundwater–surface water model. *Journal of Hydrology*, 348, 224–240.

Hoa, L.T.V., *et al*., 2008. Infrastructure effects on floods in the Mekong River Delta in Vietnam. *Hydrological Processes*, 22, 1359–1372.

Hogan, Z.S., *et al*., 2004. The imperiled giants of the Mekong. *American Scientist*, 92, 228–237.

Institute of Hydrology, 1988. *Investigation of dry season flows. Water Balance Study Phase 3.* Report to the Interim Committee for Coordination of Investigations of the Lower Mekong Basin. Wallingford: Institute of Hydrology.

Jackson, R.B., *et al*., 1996. A global analysis of root distributions for terrestrial biomes. *Oecologia*, 108, 389–411.

Johnston, R. and Kummu, M., 2012. Water resource models in the Mekong Basin: a review. *Water Resources Management*, 26, 429–455.

Kelliher, F.M., Leuning, R., and Schulze, E.D., 1993. Evaporation and canopy characteristics of coniferous forests and grasslands. *Oecologia*, 95, 153–163.

Kingston, D.G., Thompson, J.R., and Kite, G., 2011. Uncertainty in climate change projections of discharge for the Mekong River Basin. *Hydrology and Earth System Sciences*, 15, 1459–1471.

Kirby, M., *et al*., 2010. The Mekong: a diverse basin facing the tensions of development. *Water International*, 35, 573–593.

Kite, G., 2000. *Developing a hydrological model for the Mekong Basin: impacts of basin development on fisheries productivity.* Working Paper 2. Colombo: International Water Management Institute.

Lacombe, G., *et al*., 2010. Conflict, migration and land-cover changes in Indochina: a hydrological assessment. *Ecohydrology*, 3, 382–391.

Laizé, C.L.R., *et al*., 2013. Projected flow alteration and ecological risk for pan-European rivers. *River Research and Applications*, 10.1002/rra.2645.

Lauri, H., *et al*., 2012. Future changes in Mekong River hydrology: impact of climate change and reservoir operation on discharge. *Hydrology and Earth System Sciences*, 16, 4603–4619.

Li, S.J. and He, D.M., 2008. Water level response to hydropower development in the upper Mekong River. *Ambio*, 37, 170–177.

Madsen, H., 2000. Automatic calibration of a conceptual rainfall-runoff model using multiple objectives. *Journal of Hydrology*, 235, 276–288.

Maltby, E. and Acreman, M.C., 2011. Ecosystem services of wetlands: pathfinder for a new paradigm. *Hydrological Sciences Journal*, 56 (8), 1341–1359.

Marshall, T.J., Holmes, J.W., and Rose, C.W., 1996. *Soil physics.* 3rd ed. Cambridge University Press.

Mekong River Commission (MRC), 2003. *State of the basin report: 2003*. Phnom Penh: Mekong River Commission.

Millennium Ecosystem Assessment, 2005. *Ecosystems and human well-being: wetlands and water synthesis*. Washington, DC: World Resources Institute.

Nash, I.E. and Sutcliffe, I.V., 1970. River flow forecasting through conceptual models. *Journal of Hydrology*, 10, 282–290.

Nestler, J.M., *et al*., 2012. The river machine: a template for fish movement and habitat, fluvial geomorphology, fluid dynamics and biogeochemical cycling. *River Research and Applications*, 28, 490–503.

Olden, J.D. and Poff, N.L., 2003. Redundancy and the choice of hydrologic indices for characterizing streamflow regimes. *River Research and Applications*, 19, 101–121.

Poff, N.L., *et al*., 1997. The natural flow regime: a new paradigm for riverine conservation and restoration. *BioScience*, 47, 769–784.

Poff, N.L., *et al*., 2010. The Ecological Limits of Hydrologic Alteration (ELOHA): a new framework for developing regional environmental flow standards. *Freshwater Biology*, 55, 147–170.

Poff, N.L., Brinson, M.M., and Day, J.W. Jr, 2002. *Aquatic ecosystems and global climate change*. Arlington: Pew Center on Global Climate Change.

Poulsen, A.F., *et al*., 2002a. *Fish migrations of the Lower Mekong River Basin. Implications for development, planning and environmental management*. MRC Technical Paper No 8. Phnom Penh: Mekong River Commission.

Poulsen, A.F., *et al*., 2002b. *Deep pools as dry season fish habitats in the Mekong River Basin*. MRC Technical Paper No 4. Phnom Penh: Mekong River Commission.

Prudhomme, C. and Davies, H., 2009. Assessing uncertainties in climate change impact analyses on the river flow regimes in the UK. Part 2: future climate. *Climatic Change*, 93, 197–222.

Richter, B.D., *et al*., 1996. A method for assessing hydrologic alteration within ecosystems. *Conservation Biology*, 10, 1163–1174.

Richter, B.D., *et al*., 1997. How much water does a river need?. *Freshwater Biology*, 37, 231–249.

Sahoo, G.B., Ray, C., and De Carlo, E.H., 2006. Calibration and validation of a physically distributed hydrological model, MIKE SHE, to predict streamflow at high frequency in a flashy mountainous Hawaii stream. *Journal of Hydrology*, 327, 94–109.

Schultz, R.E., 1989. *ACRU: background, concepts and theory.* Report 35, Agricultural Catchments Research Unit, Department of Agricultural Engineering. Pietermaritzburg: University of Natal.

Shopea, N., 2003. *Station profiles of water quality monitoring network in Cambodia: MRC water quality monitoring station network review.* Phnom Penh: Mekong River Commission.

Simpson, B.K. and Bezuijen, M.R., 2010. Siamese Crocodile Crocodylus siamensis. *In*: S.C. Manolis and C. Stevenson, eds. *crocodiles status survey and conservation action plan*. 2nd ed. Darwin: Crocodile Specialist Group, 120–126.

Singh, C.R., *et al*., 2010. Modelling the impact of prescribed global warming on runoff from headwater catchments of the Irrawaddy River and their implications for the water level regime of Loktak Lake, northeast India. *Hydrology and Earth System Sciences*, 14, 1745–1765.

Singh, C.R., *et al*., 2011. Modelling water-level options for ecosystem services and assessment of climate change: Loktak Lake, northeast India. *Hydrological Sciences Journal*, 56, 1518–1542.

Stisen, S., *et al*., 2008. A remote sensing driven distributed hydrological model of the Senegal River basin. *Journal of Hydrology*, 354, 131–148.

Stone, R., 2010. Along with power, questions flow at Laos's new dam. *Science*, 328, 414–415.

Sverdrup-Jensen, S., 2002. *Fisheries in the lower Mekong Basin: status and perspectives.* MRC Technical Paper No. 6. Phnom Penh: Mekong River Commission.

Tharme, R.E., 2003. A global perspective on environmental flow assessment: emerging trends in the development and application of environmental flow methodologies for rivers. *River Research and Applications*, 19, 397–441.

Thompson, J.R., Green, A.J., and Kingston, D.G., 2014. Potential evapotranspiration-related uncertainty in climate change impacts on river flow: an assessment for the Mekong River Basin. *Journal of Hydrology.* doi:10.1016/j.jhydrol.2013.12.010.

Thompson, J.R., *et al*., 2004. Application of the coupled MIKE SHE/MIKE 11 modelling system to a lowland wet grassland in Southeast England. *Journal of Hydrology*, 293, 151–179.

Thompson, J.R., 2012. Modelling the impacts of climate change on upland catchments in southwest Scotland using MIKE SHE and the UKCP09 probabilistic projections. *Hydrology Research*, 43, 507–530.

Thompson, J.R., *et al*., 2013. Assessment of uncertainty in river flow projections for the Mekong River using multiple GCMs and hydrological models. *Journal of Hydrology*, 466, 1–30.

Todd, M.C., *et al*., 2011. Uncertainty in climate change impacts on basin-scale freshwater resources—preface to the special issue: the QUEST-GSI methodology and synthesis of results. *Hydrology and Earth System Sciences*, 15, 1035–1046.

Västilä, K., *et al*., 2010. Modelling climate change impacts on the flood pulse in the Lower Mekong floodplains. *Journal of Water and Climate Change*, 1, 67–86.

Vieux, B.E., 2004. *Distributed hydrologic modeling using GIS*. Dordrecht: Kluwer Academic.

Vörösmarty, C.J., *et al*., 2010. Global threats to human water security and river biodiversity. *Nature*, 467, 555–561.

WWF, 2009. *First contact in the Greater Mekong—new species discoveries*. Hanoi: World Wildlife Fund.

Wang, J.J., Lu, X.X., and Kummu, M., 2011. Sediment load estimates and variations in the lower Mekong River. *River Research and Applications*, 27, 33–46.

Welcomme, R., 2001. *Inland fisheries ecology and management*. Oxford: Blackwell Science.

Ziv, G., *et al*., 2012. Trading-off fish biodiversity, food security, and hydropower in the Mekong River Basin. *Proceedings of the National Academy of Sciences*, 109, 5609–5609.